12
Tricks of the trade

This book has largely concerned a description and explanation of the physical principles which underpin PGSE NMR. In the numerous examples presented, time-dependent magnetic field gradients are included in pulse sequences as though their role is routine, yet another facility provided by the NMR spectrometer. But in truth, the practical implementation of these sequences requires some care, an awareness of the potential role for experimental artifacts.

Consider for the moment the measurement of self-diffusion, using a typical NMR sample size of a few millimetres. The magnitude of q required to measure dynamic displacements n orders of magnitude smaller than the sample dimensions, will result in a spin dephasing of order 10^n cycles across the sample, with final rephasing in the echo required to be within a few degrees. Consequently, for a typical rms diffusion distance $\langle Z^2 \rangle^{1/2}$ on the order of 0.1 to 10 microns, the time integral of the two gradient pulses in the simple Stejskal–Tanner experiment, must be matched to better than 1 in 10^5, a demanding requirement and one that is not easily monitored by electronic means alone. In addition, if we are to effectively measure molecular displacements over micron or sub-micron distances, we had better be sure that any bulk sample movement over the echo period is significantly smaller. Yet switching magnetic fields on and off within the high polarising field results in Lorentz forces, which in turn induce mechanical motion in the gradient coils, manifest most obviously as an acoustic wave, a 'click' from the gradient coils. Can we ensure that these do not result in sample displacements that mask the underlying molecular dynamics we seek to measure?

In summary then, we need an awareness of the role of sample vibration or convective flow within our sample, of gradient pulse area matching, the role of Lorentz forces, and of eddy currents induced in surrounding conductors by time-varying magnetic fields. But more importantly we need to know how to mitigate these effects, or to avoid them completely. This chapter gives some pointers to the experimentalist that may assist in this regard. We do not seek to provide here a description of gradient coil or RF probe design, matters dealt with in the author's earlier book [1], but instead to give a short description of how to make these devices work effectively.

12.1 Instrumental limits

12.1.1 The diffusion baseline

In the measurement of diffusion, all instrumental artifacts have the effect of enhancing the diffusion coefficient. All PGSE NMR systems have a lower limit of mean-squared displacement below which artefactual attenuation exceeds diffusive attenuation. The

Translational Dynamics and Magnetic Resonance, First Edition, Paul T. Callaghan, © Paul T. Callaghan 2011.
Published in 2011 by Oxford University Press.

challenge in diffusion measurement is to ensure that instrumental factors that contribute to spin phase-spreading are kept below the spread due to diffusion alone. For example, phase instability of the spectrometer, mismatch of the gradient pulse time integrals due to current instability, or vibrations of the sample; these all contribute to additional phase spreading artifacts and so cause a measured diffusion coefficient to appear larger than its true value. In consequence, the better the instrument, the lower the value of D that may be measured. More particularly, a phase variance $\langle(\Delta\phi)^2\rangle$ gives an apparent mean-squared displacement $\langle Z^2\rangle = 2q^{-2}\langle(\Delta\phi)^2\rangle$, and an apparent diffusion coefficient $D = q^{-2}\Delta^{-1}\langle(\Delta\phi)^2\rangle$, where q is the applied wavevector and Δ the displacement observation time.

Although instrumental artifacts enhance the apparent diffusion coefficient, there does exist a sample-related artifact where one measures too small a diffusion coefficient. Such a condition can arise where internal magnetic field gradients arising from susceptibility inhomogeneity have the effect of opposing the applied gradient pulse [2, 3].

12.1.2 Test samples

An ideal sample with which to test the apparatus is one with small D and long T_2 and T_1, in other words with inhibited translational mobility and relatively free rotational mobility. Polydimethylsiloxane melts meet such requirements, but these materials have considerable chain-length polydispersity and so exhibit a wide distribution of diffusion coefficients within the same sample, leading to multi-exponential decay in the PGSE NMR experiment. For mono-disperse behaviour, semi-dilute high molecular weight polystyrene solutions are ideal, with their relatively free local segmental motion, but with entanglements highly restricting self-diffusion. For example, a 5% w/v solution of 10 MDa polystyrene in (per-deutero) toluene solvent has (for aromatic protons) $T_2 = 70$ ms and $T_1 = 800$ ms, and a self-diffusion coefficient of 6.8×10^{-16} m^{2}s^{-1} [4], at the lower limits of what can be measured using PGSE NMR. Indeed, in such a polymer the spin phase spreading can be dominated not by Brownian motion of the molecules, but by spin-diffusion, the process of magnetisation diffusion along the polymer chain caused by energy-conserving mutual spin flip-flops. The same 5% 10 MDa polymer solution yields a spin-diffusion coefficient of 3.5×10^{-15} m^{2}s^{-1} [5], and this effect must be allowed for in order to obtain the underlying polymer segmental diffusion rate.

Of course, what is directly measured in PGSE NMR is the mean-squared spin displacement $\langle Z^2\rangle$. The smallest rms distance so far measured is on the order of 25 nm, over a time Δ of around 10 ms [5]. It is this rms displacement limit with which we must compare instrumental phase errors. Note that at 10 ms such a mean-squared displacement, incorporating spin-diffusion effects, corresponds to an effective diffusion coefficient of 3×10^{-14} m^2 s^{-1} for the 5% 10 MDa polystyrene in d-toluene. The same sample returns 3.5×10^{-15} m^2 s^{-1} at Δ =1 s, (i.e. $\langle Z^2\rangle^{1/2} = 265$ nm), the diffusion coefficient discrepancy arising from polymer reptation, a dynamics which exhibits a non-Fickian, fractal $\langle Z^2(t)\rangle$ time-dependence. But for the purposes of instrument testing, the sample provides a good reference with which to probe the g, δ, and Δ parameter space of the instrument to ensure that the measured $\langle Z^2\rangle$ or D values do not exceed the known calibration values. Where these values are exceeded then the result is indicative of instrument artifact, setting a new lower limit for reliable measurement.

12.1.3 Non-Gaussian displacements

A further test of instrument reliability is to be found in the shape of the echo-attenuation data. In samples for which molecules undergo unrestricted Brownian motion, $E(q) = \exp(-\gamma^2\delta^2 g^2 D\Delta)$. A semi-log plot of echo-attenuation data allows us to test for a linear response of the exponent to $\delta^2 g^2 \Delta$ as g, δ, and Δ are independently varied. Most importantly, while deviation from linearity in the form of positive curvature can be associated with a distribution of diffusion coefficients, for example arising from molecular polydispersity, negative curvature is almost invariably another sign of instrumental artifact. Such negative curvature is often associated with increasingly incoherent signal averaging as the time integral of the pulse gradient is increased.

12.2 Conquering artifacts

Having suggested a means by which instrument artifact might be detected, we now lay out the various lines of attack whereby these unwanted phase fluctuations may be minimised. The experimenter needs to iterate amongst these avenues for improvement, using the slow diffusion sample, and the 'lowest $\langle Z^2(t)\rangle$' or 'lowest D' measure, as the indicator of success. But by far the most efficient route to a solution is by real-time monitoring of individual echoes, so that the experimenter has available an immediate visual response to any adjustment within the apparatus.

12.2.1 Real-time monitoring

Using the semi-dilute polymer sample, the spectrometer acquisition window should be set up so that a complete echo is sampled and displayed as acquired in real time. That echo should ideally be stable. Figure 12.1 shows three types of typical echo instability associated with pulsed gradient artifacts. The consequence of co-adding such unstable signals in the signal-acquisition process is a reduced signal amplitude, contributing to unphysical downward curvature in the semi-logarithmic echo-attenuation plot. By monitoring echo instability in real time, successive experimental modifications can be made and tested, the aim being to produce a consistent echo envelope, phase, and frequency.

Experimenters be warned! Modern NMR instruments permit the user to prepare many hours of automated experiments, traversing a wide range of parameter space. Failure to 'converse with the instrument', ensuring all such experiments experience stable echo conditions, can lead to the collection of worthless data.

12.2.2 Sample movement

Vibration

The most common source of echo instability is sample movement due to vibration. In instruments where the gradient coils produce a noticeable acoustic pulse on current switching, the associated vibration can easily cause sample movement relative to the gradient field. The matter of acoustic pulses and their minimisation is dealt with in the section 'small is beautiful'. But for a given coil set-up, the best remedy is to ensure that the sample is firmly inserted in the gradient/RF assembly, most easily with some Teflon tape wrapped round the glass sample tube to provide a firm fit. In systems

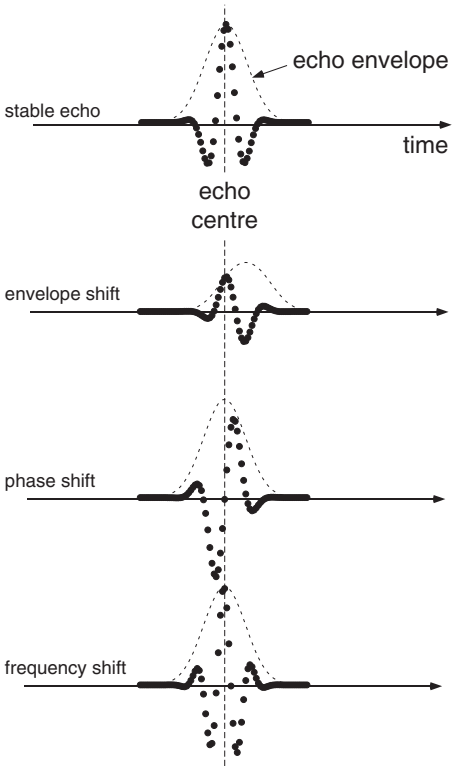

Fig. 12.1 Sequence of echoes with ideal echo at top and successively instability in the echo envelope, the echo phase, and the echo frequency. Sample movement, gradient pulse integral mismatch, and time-dependent fields due to eddy currents induced by gradient pulse switching can all contribute to a combination of these effects.

where the RF coil is free-standing with respect to the gradient coils, this may require that the tape or fixing collar is applied at a position where the sample tube is able to be directly registered with the gradient coil assembly.

This tight coupling works well for a viscous liquid sample where the relative motion of liquid and holder is strongly damped under the influence of the gradient coil acoustic pulse. However, for some samples, such as powders, the acoustic shock can cause particle jumping. Here mechanical decoupling of the sample from the gradient coil assembly can prove the most effective solution [6].

Note that many modern NMR spectrometers allow for the superconducting magnet to be raised on air-damped bearings. This can prove helpful in mitigating some vibration effects.

Convection

Whenever a liquid sample is used in the presence of a temperature gradient, convective flow is possible, an effect that plays havoc with diffusion measurements. The onset of

convection is determined by a critical balance between hydrostatic and viscous forces, as reflected by the Rayleigh–Bénard number [7, 8]

$$Ra = \frac{\alpha \Delta T g L^3}{\nu \kappa} \tag{12.1}$$

where g is the acceleration due to gravity, and α, ν, and κ are the coefficients of thermal expansion, kinematic viscosity, and thermal diffusivity of the fluid, respectively. ΔT is the vertical temperature difference across the sample and L is the thickness of the fluid layer. For a fluid of infinite horizontal extent, the critical Rayleigh–Bénard number for the onset of convection is $Ra_c \sim 1700$. However, an NMR sample is typically a vertical cylindrical tube, characterised by a radius to depth ratio, r/l, much less than one. For such a geometry, the critical value of Ra for the onset of convection is given by [9]

$$Ra_c \sim 200 \frac{l^4}{r^4} \tag{12.2}$$

For example, a 4-mm ID NMR tube with sample length 20 mm, has $r/l = 10$, which suggests a critical Ra for the onset of convection of $\sim 2 \times 10^6$. Note the dependence on the aspect ratio as the fourth power. This tells us us that an effective means of suppressing convection is to use a narrow diameter capillary. Of course many slowly diffusing systems are often highly viscous and as such, Rayleigh–Bénard convection presents no problem. But as an example, consider the polymer system 5% w/w $M_w = 127,000$ Da polystyrene/cyclohexane solution, studied by Manz *et al.* [10], for which the polymer solution viscosity is $\eta = 1.43 \times 10^{-3}$ Pa s, close to that of water. For a 25-mm length sample, with 3.0-mm ID, Ra_c for the onset of convection $\sim 10^7$. Using the literature values of α and κ, this value of Ra occurs at a temperature difference from top to bottom of 4 K.

12.2.3 Eddy currents

Throughout this book we have represented gradient pulses as schematic rectangles, implying in the process an infinite rate of rise and fall of gradient currents and associated field. Of course, such a simplistic representation is impossible in practice. The maximum current switching speed, di/dt, is partly limited by the power-supply voltage, which must equal $Ri + Ldi/dt$ where L is the load inductance and R the load resistance. The other limitation is the power-supply bandwidth, expressed in the time domain as a 'slew rate' or maximum rate of change of current. And even if our power supply were able to deliver high slew rates, there is another reason why we would wish to limit the rate of rise and fall of our gradient current pulses. The rapidly changing magnetic fields arising from the gradient pulse switching interact with surrounding metal to induce eddy currents proportional to the current switching rate, di/dt, and these currents in turn have associated magnetic fields, which not only distort the gradient profiles around the sample but also can persist for tens of milliseconds after the gradient pulse has been turned off. While these 'eddy gradients' are not such a severe problem in the electromagnet, where the pole pieces present an unfavourable geometry for current flow, in the superconducting solenoid with its cylindrical tubes

of surrounding metal these currents can be devastating in their effect. For this reason PGSE NMR systems in superconducting magnets benefit from the largest possible diameter bore space.

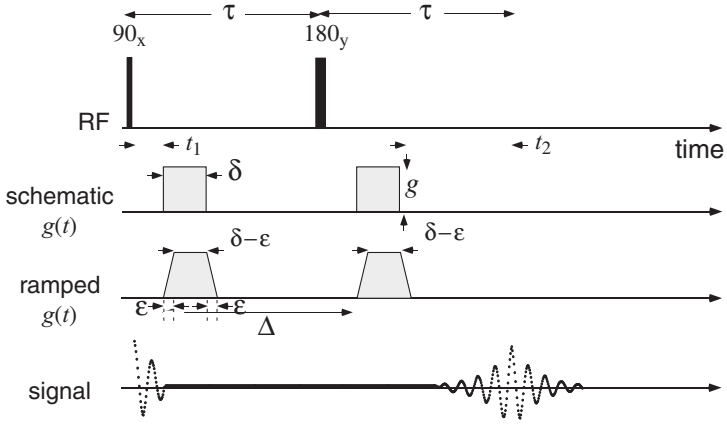

Fig. 12.2 Simple Stejskal–Tanner PGSE NMR sequence showing idealised rectangular gradient current pulses, along with a practical ramped alternative, designed to reduce the effect of eddy-current-induced field distortions.

Unless the gradient coils are much smaller than the magnet bore, some manner of eddy gradient compensation or suppression is essential. The simplest remedy is to ramp the rise and fall of the current pulses as shown in Fig. 12.2, with typical rise times, ϵ, of a few tens of microseconds often being sufficient to mitigate any noticeable eddy-current problems. Again, the best diagnostic is to monitor the real-time echo stability while the pulse rise time is adjusted. Note that the shift to a trapezoidal pulse shape implies a slight (but often insignificant) change to the Stejskal–Tanner expression for the echo attenuation, as outlined in Section 5.5.1.

There does exist another approach to eddy-current-induced field compensation, through what is known as 'pre-emphasis' and 'de-emphasis' of the coil current, a process that relies on Lenz's law requirement that the sign of fields associated with eddy currents will be opposed to the change that produced them. By deliberately overdriving the current at the leading and falling edges, the coils themselves produce fields that compensate the unwanted induced gradients. The optimisation of pre-emphasis and de-emphasis currents is a complex process, requiring adjustment of a multitude of time constants and of amplitudes for exponential currents, which are added to the desired waveform. This compensation can never be perfect since the spatial distribution of the additional fields produced by the gradient coils will never match those produced by current in the surrounding metal.

The best philosophy is to ensure eddy gradient suppression by using gradient sets the fields of which are zero outside the coil boundaries. Active shielding [1, 11] involves adding a second layer of current density outside the primary coil surface, in a design intended to compensate the primary coil field at all points in space outside the screen.

Because this approach is so successful at removing eddy current effects without the need for pre-emphasis or de-emphasis pulse shaping, it provides a means of generating rapidly switched gradient pulses in which ease of use is traded against complexity in coil design.

12.2.4 Pulse mismatch

The stability of the gradient-current supply sets the ultimate capability of the PGSE NMR experiment. k-space encoding merely requires that we provide a suitable integral of current through the gradient coils, to a precision and accuracy consistent with the desired spatial resolution, measured as a fraction of sample dimension and possibly on the order of 0.5%. By contrast, in q-space applications the need to control current pulse integral is considerably more stringent. In these experiments we may be seeking to measure sub-micron displacements with sample dimensions of several millimetres, thus demanding gradient pulse balance better than 10^{-5}. Ripple or noise on a current supply at these low levels is extremely difficult to observe directly via an oscilloscope. Indeed, the very best sensor for current quality will be the real-time PGSE NMR measurement.

Mains hum

First and foremost, the matter of mains 'hum' needs to be attacked. Any ripple due to residual AC components in the current supply will cause gradient pulse mismatch. This will be at a maximum when the separation Δ between the pulses is half a mains cycle, it will fluctuate when Δ is incommensurate, and will be minimised when Δ is exactly equal to a mains cycle. Mains frequencies are either 50 Hz or 60 Hz depending in which part of the world one is operating. Alternate Δ between an incommensurate value and 20 ms (50 Hz) or 16.67 ms (60 Hz), and look for an improvement in the echo stability. If such improvement exists, your power supply is inadequate to the task and unless you can reduce the ripple you may be condemned to only be able to use Δ values that are a multiple of the mains period. A feasible solution, which allows greater timing freedom, is to use a 'mains trigger" to set the pulse sequence timing [12]. This ensures a fixed gradient pulse integral mismatch at any particular separation Δ, a discrepancy which can be compensated by a small adjustment in the second gradient pulse duration or by means of a stabilising background gradient (see section 12.3.3).

Power-supply 'sagging'

Even the best power supply will have limits to its ability to supply transient power output at a consistent value. After any recovery period the first pulse will typically deliver a little more power than the succeeding. However, there will exist a steady-state output level in a repetitive train where the pulses deliver close to equal power. The trick, therefore, is to run the power supply using a train of 'dummy' pulses that have no influence on the spin system, selecting for the actual PGSE NMR measurement pulses later in the train when the power supply has settled. The idea is illustrated in Fig. 12.3.

Gradient pulse compatibility with power supply

The gradient $g(t)$ is commonly generated using a current $i(t)$ from a current source, a high-power operational amplifier driven in a current-controlled mode. This control

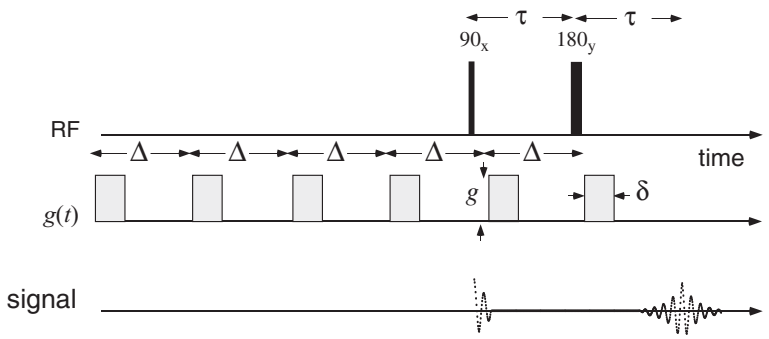

Fig. 12.3 Simple Stejskal–Tanner PGSE NMR sequence in which a train of 'dummy' gradient current pulses is applied prior to excitation by the 90°_{x} RF pulse. By ensuring equal spacing between all the gradient pulses, the power supply settles to a steady-state power output value before the final pulse pair comprising the actual measurement.

is achieved using a feedback loop involving a sensing resistor. The operational amplifier compares the voltage measured across this resistor with a voltage function $v(t)$, representing the the desired time-dependence of the gradient pulse. Stallmach and Galvosas [13] have pointed out that if the rise or fall rate of the gradient current pulse is set too high, the voltage across the coil may exceed the maximum DC voltage of the power supply, v_B. When this happens, proper current control is lost and error currents caused by the ripple, hum, and noise of the DC power supply will be unsuppressed by the feedback loop to the gradient current. These authors point out that by optimally shaping the gradient current pulse using an appropriate setpoint function, $v(t)$, such overloads can be avoided. The best shape for maximum pulse-switching speed is an exponential growth controlled by the coil time constant L/R, where L and R are the coil inductance and resistance, respectively, and where the maximum slew rate is limited to v_B/L.

12.2.5 Small is beautiful

Given the opportunity to design and build one's own gradient coil, it is worth noting that most of the artifacts discussed in this chapter can be considerably alleviated by choosing to use the smallest practicable gradient coil assembly [14]. Downsizing leads to reduced coil inductance and hence reduced power-supply requirements. Most importantly, there will be the reduced Lorentz torque on the coil array and consequently less acoustic response and sample vibration. In addition, there will of course be significantly reduced induction of eddy currents in the surrounding magnet due to stray pulsed magnetic fields, in particular because a gradient coil comprises an opposed pair of dipoles and therefore represents an octopole the stray fields of which attenuate with distance r as $(r/a)^{-5}$, where a is the radius of the coil. Finally, a small gradient coil implies a smaller sample volume. While there is a signal-to-noise price to be paid, smaller sample volumes both inhibit convection and lead to a less stringent requirement for

gradient pulse time integral matching, since the area mismatch results in a dephasing error proportional to the sample dimensions.

12.2.6 Fringe field diffusometry

A particularly effective means of avoiding most problems associated with gradient pulse mismatch, eddy currents, and sample movement is to avoid the use of current-switched pulsed gradients altogether. Kimmich and co-workers [15] suggested using the fringe field of a superconducting magnet to provide very high constant magnetic field gradients, on the order of 10 T/m, which can be turned into pulses of the effective gradient by means of a stimulated-echo RF sequence. The idea is shown in Fig. 12.4.

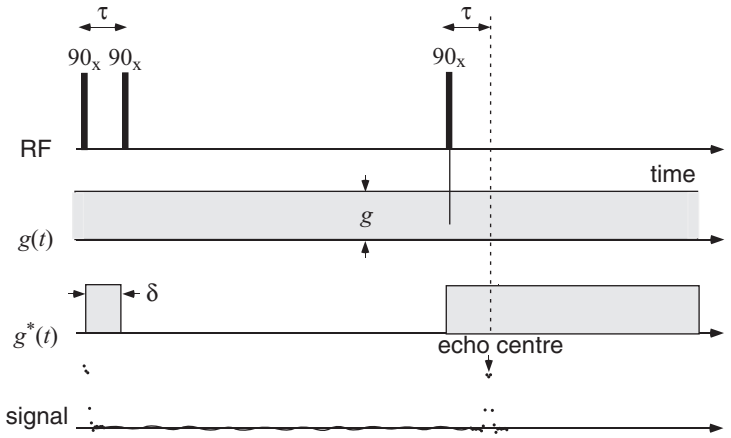

Fig. 12.4 Fringe field diffusometry pulse sequence in which a stimulated echo is used in the presence of a constant strong magnetic field gradient to create an effective gradient sequence, which appears to the spins as pulses. Note that the 90°_x RF pulses are slice selective and that the signal in the frequency domain is related to the RF pulse spectrum, so that the time-domain signal is reminiscent of the RF pulse shape.

The great advantage of the method is that, unlike gradient fields produced by pulsing current through coils, the highly stable superconducting fringe field of the magnet has practically no discernable temporal fluctuation and induced-eddy-current effects are absent because the formation of effective gradient pulses is via the 'framing' action of the RF pulses on the constant gradient. The disadvantages of the fringe field method are, first, that spectral resolution is lost by the need to detect the signal in the presence of the constant gradient and, second, that because of the spectral spread associated with the constant gradient, the signal is weak, the RF pulses being inevitably slice-selective, exciting spins residing only within their bandwidth. Even with high-power RF, and hence brief wide-bandwidth pulses, a typical sample slice contributing to the experiment might be on the order of 100 microns thick. These disadvantages are no particular handicap where one is working with a single dominant molecular species at

high concentration, for example in studying the diffusion of polymer melts [16] or the restricted diffusion of a mono liquid in a porous matrix [17].

12.3 Pulse-sequence compensation

Having optimised the apparatus, there do exist pulse-sequence design strategies that can further compensate for remaining artifacts, including those caused by eddy-current-induced fields, convection, sample movement, and gradient pulse mismatch.

12.3.1 Eddy current fields

One of the problems associated with eddy currents in the magnet assembly induced by the switching of gradient pulses concerns the persistence of time-dependent fields which perturb the spectral resolution during signal acquisition. To assess the effect of eddy fields, an ideal test is to apply a gradient pulse followed by a variable delay time before an excitation 90° RF pulse and signal acquisition, as shown in Fig. 12.5. As the delay is increased, allowing for eddy-field decay, the experimenter gains insight regarding the longevity of these fields by examining the gradual improvement of the NMR spectrum quality.

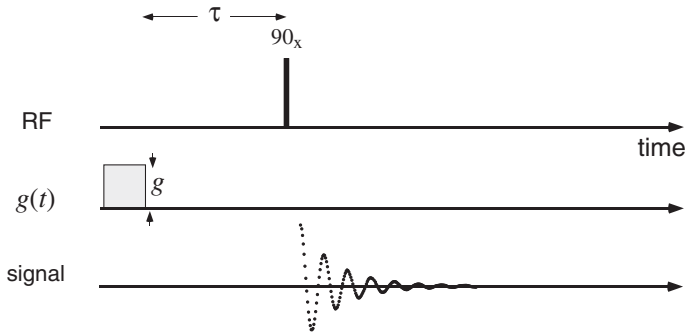

Fig. 12.5 Simple excitation and acquire RF pulse sequence, in which the 90° RF pulse is preceded by a gradient pulse and a variable delay. As the delay is increased, the decay of eddy fields results in decreasing spectral distortion. By this means decay time constants can be established.

A simple solution is the longitudinal eddy current decay (LED) method of Gibbs and Johnson [18], in which the magnetisation at the echo formation is stored along the longitudinal axis by means of 90° RF pulses, as shown in Fig. 9.14. During the storage period, τ_e, the unwanted fields can be allowed to attenuate before recall of the magnetisation for readout using a second 90° RF pulse. Clearly T_1 provides an upper limit for the time over which such storage is possible, and a suitable phase-cycling scheme is needed to ensure that only magnetisation arising from the initial excitation pulse contributes to the final signal.

12.3.2 Convection compensation

Inhibiting convection by restricting sample dimensions comes at the price of a loss of signal. An alternative strategy is to utilise flow compensation methods to remove unwanted phase shifts due to convective flow in the sample [19]. These are effective only if the convective flow is laminar and constant over the timescale of the flow-compensated PGSE gradient sequence. Where the convective flow fluctuates over the duration of the gradient pulse train, or where turbulence is present, the method cannot work effectively. However, many practical examples of convective flow driven by small temperature gradients across the sample do exhibit the necessary stability. Figure 5.11(b) shows an effective gradient sequence resulting in the echo condition $\int_0^t g^*(t')dt' = 0$, but with first moment $\int_0^t t'g^*(t')dt'$ zero, thus resulting in insensitivity to flow.

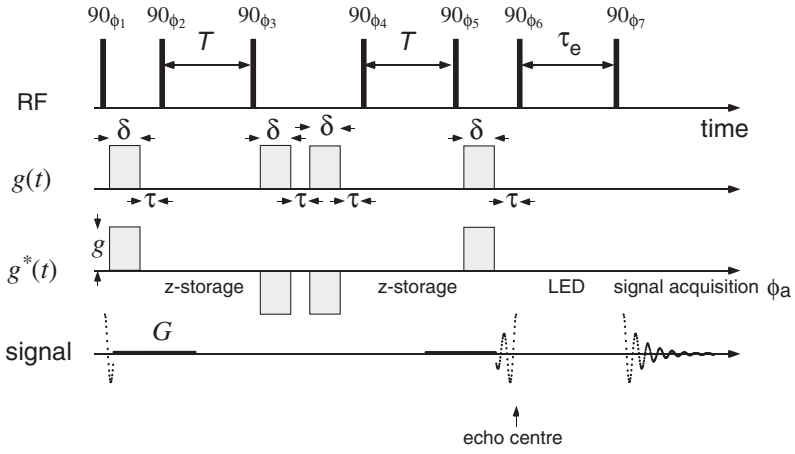

Fig. 12.6 Double stimulated-echo PGSE NMR sequence with zero first moment of the effective gradient, as suggested by Jerschow and Mueller, in which an LED segment (duration τ_e) is used to allow for the decay of fields associated with induced eddy currents. The phase cycle is $\phi_1 = x, y, -x, -y$; $\phi_2 = \phi_5 = \phi_6 = \phi_7 = x$; $\phi_3 = -x, -y$; $\phi_4 = 4(-x), 4(x)$; $\phi_a = x, x, -x, -x, -x, -x, x, x$. Homospoil gradients should be applied during the z-storage intervals. (Adapted from Jerschow and Müller [19].)

Figure 12.6 shows an example of a flow-compensated PGSE NMR sequence [19] based on a double stimulated echo, for which the echo-attenuation expression is given by

$$E(q) = \exp\left(-q^2(T + \frac{4\delta}{3} + 2\tau)\right) \tag{12.3}$$

where $q = \gamma g\delta$. This is but one of a set of sequence options. Further examples are provided in references [20–22]. Note that one of the consequences of convection-compensating sequences is the lack of clear definition of the time over which diffusion occurs. This presents no disadvantage in the case of unrestricted free diffusion, where an exact expression for the echo attenuation is available. And, in the case of samples

exhibiting restricted diffusion, where we seek a definitive timescale, the problem of convective perturbation is unlikely to arise.

However, there is a highly effective means of avoiding convection problems while retaining sensitivity to timescale-dependent diffusivity, and that is to shift to frequency-domain analysis using the CPMG methodology outlined in Section 5.7.2. Here flow effects are completely suppressed over the period T of the effective gradient cycle, while restricted diffusion can be studied by probing the diffusion spectrum through the gradient waveform frequency sweep.

12.3.3 Gradient pulse mismatch compensation

The effects of sample movement and gradient-pulse mismatch are exhibited in the echo phase of the PGSE NMR experiment. Movement results in a phase shift common to all spins, while mismatch results in position-dependent local phase shifts. If the entire sample moves by $\Delta\mathbf{r}$ between the first and second pulses, while the gradient mismatch is given by $\Delta\mathbf{q}$, then the narrow gradient pulse equation 5.85 must be rewritten

$$E(\mathbf{q},\Delta) = \int \overline{P}(\mathbf{R},\Delta)\exp(i\mathbf{q}\cdot\mathbf{R}+\Phi)d\mathbf{R}, \tag{12.4}$$

where

$$\mathbf{q}\cdot\mathbf{R}+\Phi = (\mathbf{q}+\Delta\mathbf{q})\cdot(\mathbf{r}+\mathbf{R}+\Delta\mathbf{r}) - \mathbf{q}\cdot\mathbf{r} \tag{12.5}$$

We shall only be concerned with sample motion displacements Δz parallel to $\mathbf{q}$ and will presume that these are common to all spins in the sample. This 'rigid body' assumption is reasonable if the material being studied is sufficiently viscous that we wish to observe very slow motion. Noting further that Δq is parallel to $\mathbf{q}$,

$$\begin{aligned} E(q,\Delta) = \{&\int \overline{P}(Z,\Delta)\exp(iqZ)dZ\} \\ &\times\{\exp[i(q+\Delta q)\Delta z]\} \\ &\times\{\int \rho(z)\exp(i\Delta qz)dz\} \end{aligned} \tag{12.6}$$

The first bracketed term in eqn 12.6 is the Fourier transform of the average propagator, the quantity that contains the information about microscopic dynamic displacements. It is sensible to label this term $E_0(q,\Delta)$, representing the unperturbed echo attenuation that we seek to measure. The second term is a phase shift resulting from net motion of the sample, caused, for example, by vibration. The final term is the integral of position-dependent phase shifts and is clearly reminiscent of k-space encoding. While the second term could be removed by autophasing or modulus calculation, the third is only amenable to correction once the spatial dependence of the phase shifts is unravelled. This can be achieved by means of a read gradient, as shown in Fig. 12.7. Of course, the price paid is that NMR spectral resolution is lost. Hence the method is really only applicable when we are able to uniquely identify the deliberately broadened NMR spectrum with the desired molecular species.

By using the same gradient coil responsible for pulse mismatch in g to generate a much smaller read gradient G, the phase shifts can be resolved. Given pixels separated

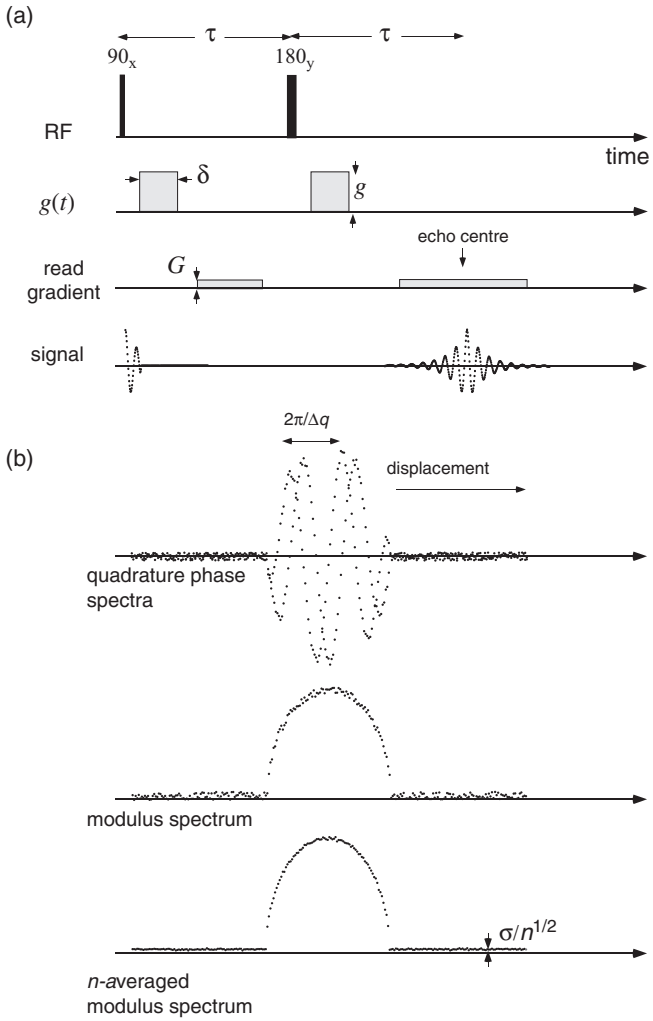

Fig. 12.7 (a) PGSE-MASSEY pulse sequence with q-gradient pulses (amplitude g) and k-gradient pulses (amplitude G). The read gradient enables the restoration of spatially dependent phase shifts at a time $-\Delta q/\gamma G$ with respect to the echo centre. (b) Simulated data for a PGSE experiment in which a q-pulse mismatch is present. The spatially dependent phase shift (fluctuating spatial period $2\pi/\Delta q$) is revealed by Fourier transformation of the signal acquired in the presence of a read gradient generated with the same coil. The phase artifacts are removed by taking the modulus of the spectrum.

by $1/NT$ it is clear that we require $G > \Delta q/\gamma NT$. Where Δq arises from a gradient fluctuation, Δg, G will need to be comparable with this difference. Note that the effect of the read gradient in the pulse sequence shown in Fig. 12.7 is to cause a coherent superposition at the instant $t = -\Delta q/\gamma G$, arising either before or after the expected

echo centre depending on the sign of the mismatch. If G is made very large then the echo may be 'centred' by brute force, although this will result in a wide spectral spread and consequent signal-to-noise ratio reduction. The best result is obtained by Fourier transforming the echo signal with respect to k where $k = \gamma Gt$. This yields

$$E(q, \Delta) = E_0(q, \Delta)\{\exp[i(q + \Delta q)\Delta z]\ \rho(z) \exp(i\Delta q z)\} \tag{12.7}$$

The result of this transformation is shown in Fig. 12.7(a). Provided that the entire echo is sampled, $E_0(q, \Delta)$ can be recovered by computing the spectrum modulus, so that signal averaging can then proceed despite the fact that Δz and Δq may fluctuate from one acquisition to the next.

The process of signal averaging under power spectrum addition is easily represented, given a spectrum area A corresponding to the echo centre amplitude. For n acquisitions (labelled by i) and with m pixels (labelled by j), the power sum of the signal a_j and noise σ_{ij} in pixel j is

$$power(j) = \sum_{i=1}^{n} (a_j + \sigma_{ij})^2 = na_j^2 + n\sigma^2 + 2a_j \sum_{i=1}^{n} \sigma_{ij} \tag{12.8}$$

where σ is the rms noise per pixel. The term $n\sigma^2$ is the noise power baseline and can be easily calculated (from data points outside the spectrum) and subtracted. Following this the net power is given by

$$power(j) = na_j^2(1 + 2\sigma_j / n^{1/2} a_j) \tag{12.9}$$

σ_j being a noise amplitude with the same rms value, σ. The second term in the parentheses may be made arbitrarily small by averaging with n sufficiently large. Thus, using the binomial approximation, the square root of the power in pixel j is simply $n^{1/2}a_j + \sigma_j$ and the integral over the spectrum is

$$signal = n^{1/2} A + \sum_{j=1}^{m} \sigma_j \tag{12.10}$$

The noise sum is a random value centred about zero and with standard deviation $m^{1/2}\sigma$. In consequence the overall signal-to-noise ratio is $n^{1/2}A/m^{1/2}$, which represents a degradation by a factor $m^{1/2}$ compared with the case where no read gradient is employed. The use of a read gradient coupled with modulus-squared spectral addition has been dubbed PGSE-MASSEY [23] for Modulus Addition using Spatially Separated Echo spectroscopY.

The loss of signal-to-noise ratio by $m^{1/2}$ represents a very small price to be paid for the gain in PGSE resolution. For example, at the q-value where mismatch effects become important, an increase in q by 100 requires spectral-spatial spreading into 100 pixels, degrading the signal-to-noise ratio by 10. In many interesting applications, such as investigation of internal motion in high polymer melts, the PGSE experiment is frustrated by phase instability alone, and the facility to probe dynamic displacements on a distance scale of 1 to 10 nm, some two orders of magnitude lower than existing limits, is well worth the loss of a factor of ten in signal sensitivity.

12.3.4 Varying q

In varying the magnitude of the q-vector in PGSE NMR, either the gradient pulse amplitude g or the pulse duration δ may be swept. Clearly, g variation provides better time-definition of the pulse and allows one to fix the pulse duration to conditions where the 'narrow gradient pulse approximation' applies. Apart from these factors there is no reason why either g or δ might not be used as the control parameter for the experiment, and both approaches are used with equal success.

One particularly interesting aspect of g variation is the ease of traversing both negative and positive q-space, according to the sign of the current through the gradient coil. In the measurement of displacement propagators, the ability to sample the signal response to a sweep of both negative and positive q-domains confers particular advantage in that the propagator will have no dispersion component. This greatly simplifies the delicate task of 'phasing the spectrum', a process which can be a bit arbitrary when the propagator is broad, by simply seeking the imaginary spectrum null or, in a brute force manner, by calculating the modulus of the complex spectrum. Displacement propagators are invariably better represented when both signs of q-space are sampled.

12.4 Final thoughts

This chapter briefly summarises some of the better understood problems of practical implementation associated with PGSE NMR. The relative importance of each of these will depend on the particular apparatus. With awareness raised, the experimenter needs to explore the parameter space of the instrument and determine the boundaries beyond which dragons lie.

In the case of diffusion measurement, mere appearance of the echo signal as a Gaussian echo decay is no guarantee of a well-functioning experiment. Cruelly, many stochastic phase fluctuations unrelated to molecular translation will mimic just such an apparent adherence to the Stejskal–Tanner formula. Ultimately, there is no substitute for real understanding of the intrinsic physics and vigilant scepticism on the part of the experimenter, who should always verify the domain of measurement using a known diffusion coefficient for calibration.

By comparison with PGSE NMR, MRI is a safer method, plagued by fewer experimental difficulties. The reasons should be abundantly clear. In the measurement of translational dynamics by magnetic resonance, we traverse three to four orders of magnitude of translation time (milliseconds to tens of seconds), and, potentially, an even greater number of decades of translation distance (10 nm to 10 mm). There is nothing 'routine' about this remarkable experimental tool, nothing that permits the 'press of a button' and the delivery of a meaningful number, except where we confine the operator to a limited and well-proven domain. Yet, with care, calibration, and craft, good experimentalists have successfully used this method right to the edge of 'dragon lands', and done so with accuracy and precision. The key to success is physical insight and understanding. Hopefully, this book will contribute in some small measure to advancing those virtues.

References

[1] P. T. Callaghan. *Principles of Nuclear Magnetic Resonance Microscopy.* Oxford, New York, 1991.

[2] J. Zhong, R. P. Kennan, and J. C. Gore. Effects of susceptibility variations on NMR measurements of diffusion. *J. Magn. Reson.*, 95:267, 1991.

[3] S. Vasenkov, P. Galvosas, O. Geier, N. Nestle, F. Stallmach, and J. Kärger. Determination of genuine diffusivities in heterogeneous media using stimulated echo pulsed field gradient NMR. *J. Magn. Reson.*, 149:228, 2001.

[4] M. E. Komlosh and P. T. Callaghan. Segmental motion of entangled random coil polymers studied by pulsed gradient spin echo nuclear magnetic resonance. *J. Chem Phys*, 109:10053, 1998.

[5] M. E. Komlosh and P. T. Callaghan. Spin diffusion in semi-dilute random coil polymers studied by PGSE NMR. *Macromolecules*, 33:6824, 2000.

[6] N. K. Bar, J. Kärger, C. Krause, W. Schmitz, and G. Seiffert. Pitfalls in PFG NMR self-diffusion measurements with powder samples. *J. Magn. Reson. A*, 113:278, 1995.

[7] H. Bénard. Les tourbillons cellulaire dans une nappe liquide transportant de la chaleur par convection en regime permanent. *Annals Chim. Phys.*, 11:1261, 1900.

[8] Lord Rayleigh. On convective currents in a horizontal layer of fluid when the higher temperature is on the underside. *Phil. Mag.*, 32:529, 1916.

[9] G. S. Charlson and R. L. Sani. On convective instability in a bounded cylindrical fluid layer. *Int. J. Heat and Mass Transfer*, 14:2157, 1971.

[10] B. Manz, J. D. Seymour, and P. T. Callaghan. PGSE NMR observations of convection. *J. Magn. Reson.*, 125:153, 1997.

[11] P. Mansfield and B. Chapman. Active magnetic screening of coils for static and time-dependent magnetic field generation in NMR imaging. *J. Phys. E.: Scient. Instrum.*, 19:540, 1986.

[12] P. Galvosas, F. Stallmach, G. Seiffert, J. Kaerger, U. Kaess, and G. Majer. Generation and application of ultra-high-intensity magnetic field gradient pulses for NMR spectroscopy. *J. Magn. Reson.*, 151:260, 2001.

[13] F. Stallmach and P. Galvosas. Spin echo NMR diffusion studies. *Ann. Reports on NM Spectroscopy*, 61:52, 2007.

[14] P. T. Callaghan, M. E. Komlosh, and M. Nyden. High magnetic field gradient PGSE NMR in the presence of a large polarizing field. *J. Magn. Reson.*, 133:177, 1998.

[15] R. Kimmich, W. Unrath, G. Schnur, and E. Rommel. NMR measurement of small self-diffusion coefficients in the fringe field of superconducting magnets. *J. Magn. Reson.*, 91:136, 1991.

[16] E. Fischer, R. Kimmich, and N. Fatkullin. NMR field gradient diffusometry of segment displacements in melts of entangled polymers. *J. Chem. Phys.*, 104:9174, 1996.

[17] E. Farrhar, I. Ardelean, and R. Kimmich. Probing four orders of magnitude of the diffusion time in porous silica glass with unconventional NMR techniques. *J. Magn. Reson.*, 182:215, 2006.

[18] S. J. Gibbs and C. S. Johnson. A PFG NMR experiment for accurate diffusion and flow studies in the presence of eddy currents. *J. Magn. Reson.*, 93:395, 1991.

[19] A. Jerschow and N. Müller. Suppression of convection artifacts in stimulated-echo diffusion experiments. Double-stimulated-echo experiments. *J. Magn. Reson.*, 125:372, 1997.

[20] A. Jerschow and N. Müller. Convection compensation in gradient enhanced nuclear magnetic resonance spectroscopy. *J. Magn. Reson.*, 132:13, 1998.

[21] J. Krane J. G. H. Sorland, J. G. Seland and H. W. Anthonsen. Improved convection compensating pulsed field gradient spin-echo and stimulated-echo methods. *J. Magn. Reson.*, 142:323, 2000.

[22] K. I. Momot and P. W. Kuchel. Convection-compensating PGSE experiment incorporating excitation-sculpting water suppression (CONVEX). *J. Magn. Reson.*, 169:92, 2004.

[23] P.T. Callaghan. PGSE-MASSEY, a sequence for overcoming phase instability in very high gradient spin echo NMR. *J. Magn. Reson.*, 88:493, 1990.